Contract # NNX11AC17G Project # 3506G62/RB462

The Final report for ESTIMATING THE TROPOSPHERIC BRO BUDGET FROM SATELLITE MEASUREMENTS AND IMPROVING RETRIEVALS OF TROPOSPHERIC BRO VERTICAL COLUMN DENSITIES

Publication resulted from this project:

Analysis of satellite-derived Arctic tropospheric BrO columns in conjunction with aircraft measurements during ARCTAS and ARCPAC, S. Choi, Y. Wang, R. J. Salawitch, T. Canty, J. Joiner, T. Zeng, T. P. Kurosu, K. Chance, A. Richter, L. G. Huey, J. Liao, J. A. Neuman, J. B. Nowak, J. E. Dibb, A. J. Weinheimer, G. Diskin, T. B. Ryerson, A. da Silva, J. Curry, D. Kinnison, S. Tilmes, and P. F. Levelt, 2012, Atmos. Chem. Phys., 12, 1255-1285, 2012, www.atmos-chem-phys.net/12/1255/2012/, doi:10.5194/acp-12-1255-2012

Here, we report the highlights of the published results and preliminary results.

## 1. Introduction

Bromine radicals (BrOx = Br + BrO) are important species owing to their ability to destroy ozone catalytically [Barrie et al., 1988]. They may also impact oxidative pathways of many trace chemicals including mercury [Schroeder et al., 1998], and dimethyl sulfide (DMS) [Toumi , 1994]. For example, bromine radicals are known to oxidize gaseous elemental mercury (GEM) to reactive gaseous mercury (RGM) [Schroeder et al., 1998]. Rapid depletion of GEM concurrent with high BrO concentrations has been reported in the polar boundary layer [Ariya et al., 2004] as well as in the tropical marine boundary layer [Saiz-Lopez et al., 2006]. In addition, bromine radicals oxidize DMS which may shift the DMS oxidation channel [Read et al.,, 2008, Mahajan et al.,, 2010, Saiz-Lopez et al., 2004, 2006]. DMS oxidation is normally dominated by OH, particularly in tropical marine boundary layer. However, high BrO concentrations can cause DMS oxidation to be dominated by BrO. This in turn may affect aerosol formation and cloud albedo [von Glasow and Crutzen., 2004]. Therefore bromine radicals could inuence global climate through the production of cloud condensation nuclei [Read et al.,, 2008].

Bromine monoxide (BrO) is the most commonly observed active bromine species. BrO absorbs ultraviolet (UV) radiation, which enables measurement using remote sensing techniques. Space-based observation observations of BrO provide global coverage, far superior to the spatial coverage available from ground- and aircraft-based measurements. Nadir-viewing instruments on polar-orbiting satellites provide multiple daily observations of total column BrO.

Chance [1998] and Hegels et al. [1998] retrieved BrO total vertical column densities (VCD) from nadir radiances in the UV obtained by Global Ozone Monitoring Experiment (GOME) on the European

Space Agency (ESA) European Remote Sensing 2 (ERS-2) satellite. The early GOME observations showed large enhancements over Hudson Bay during spring 1997, which was attributed to bromine release from the surface [Chance, 1998]. Estimates of BrO total column amount have been subsequently derived from other nadir-viewing satellite sensors including the Ozone Monitoring Instrument (OMI) [Levelt et al., 2006] on the US National Aeronautics and Space Administration (NASA) Aura satellite, SCIAMACHY [Bovensmann et al., 1999] on the ESA Environmental Satellite (EnviSat), and the second Global Ozone Monitoring Experiment (GOME-2) instruments [Munro et al., 2006] that are flying on the series of European Meteorological Operational Satellites (EuMetSat MetOp). Retrievals of VCD BrO from different satellite instruments and by various groups tend to be in fairly close agreement.

Tropospheric BrO columns can be derived from satellite observations using the residual method, in which an estimate of the stratospheric BrO column is subtracted from the satellite-derived VCD of BrO. Wagner and Platt [1998] and Richter et al. [1998] estimated tropospheric VCD of BrO using this approach from GOME observations, based on simple assumptions for stratospheric BrO. These studies and many others assumed that stratospheric BrO is zonally symmetric and that bromine was supplied to the stratosphere solely by the decomposition of long-lived organic compounds. Theys et al. [2009] and Salawitch et al. [2010] showed that the stratospheric VCD of BrO can exhibit strong gradients with respect to longitude at high latitude during spring and Salawitch et al. [2010] questioned prior estimates of residual tropospheric BrO found assuming that the stratospheric burden was zonally symmetric. Theys et al. [2011] derived tropospheric BrO columns from GOME-2 spectra with a model-based stratospheric BrO climatology [Theys et al., 2009] similar to that used here and described in Section 2.

## 2. Validation of OMI tropospheric column BrO

We derive tropospheric vertical column densities (VCDs) using BrO total slant column densities (SCD) retrieved from OMI and a model simulation of the stratospheric BrO column. Detailed explanation to derive the tropospheric column BrO is described in Choi et al. [2012]. We compare the tropospheric BrO VCD with tropospheric BrO columns are inferred from aircraft measurements of in-situ BrO obtained during the NASA Arctic Research of the Composition of the Troposphere from Aircraft and Satellite (ARCTAS) campaign.

We find good agreement between the satellite-derived tropospheric BrO VCD and the aircraft measurement on 17 Apr 2008. Figure 1 shows time series plots of DC-8 flight data and collocated satellite measurements on 17 April 2008. This figure is from Choi et al. [2012]. We indicate time in hours relative to the starting date of the flight; therefore times greater 24:00 refer to the following day. DC-8 data include aircraft altitude, in-situ O3, CO, BrO, active bromine and soluble bromide. Satellite data include OMI-derived BrO columns (total and tropospheric), the difference between the effective cloud pressure and the terrain pressure (which indicates shielding from clouds), OMI 331nm reflectivity, and Aqua MODIS cloud optical thickness. Estimated errors of satellite-derived BrO columns are presented as vertical error bars.

The tropopause height, as given in the MERRA data set, is at approximately 7km during the flight (not shown). CO and O3 data suggest that there were no stratospheric intrusions for any of the collected tropospheric BrO profiles. Obvious signatures of stratospheric air (low CO and high O3) were occasionally seen, but only when the aircraft was flying near or above the tropopause.

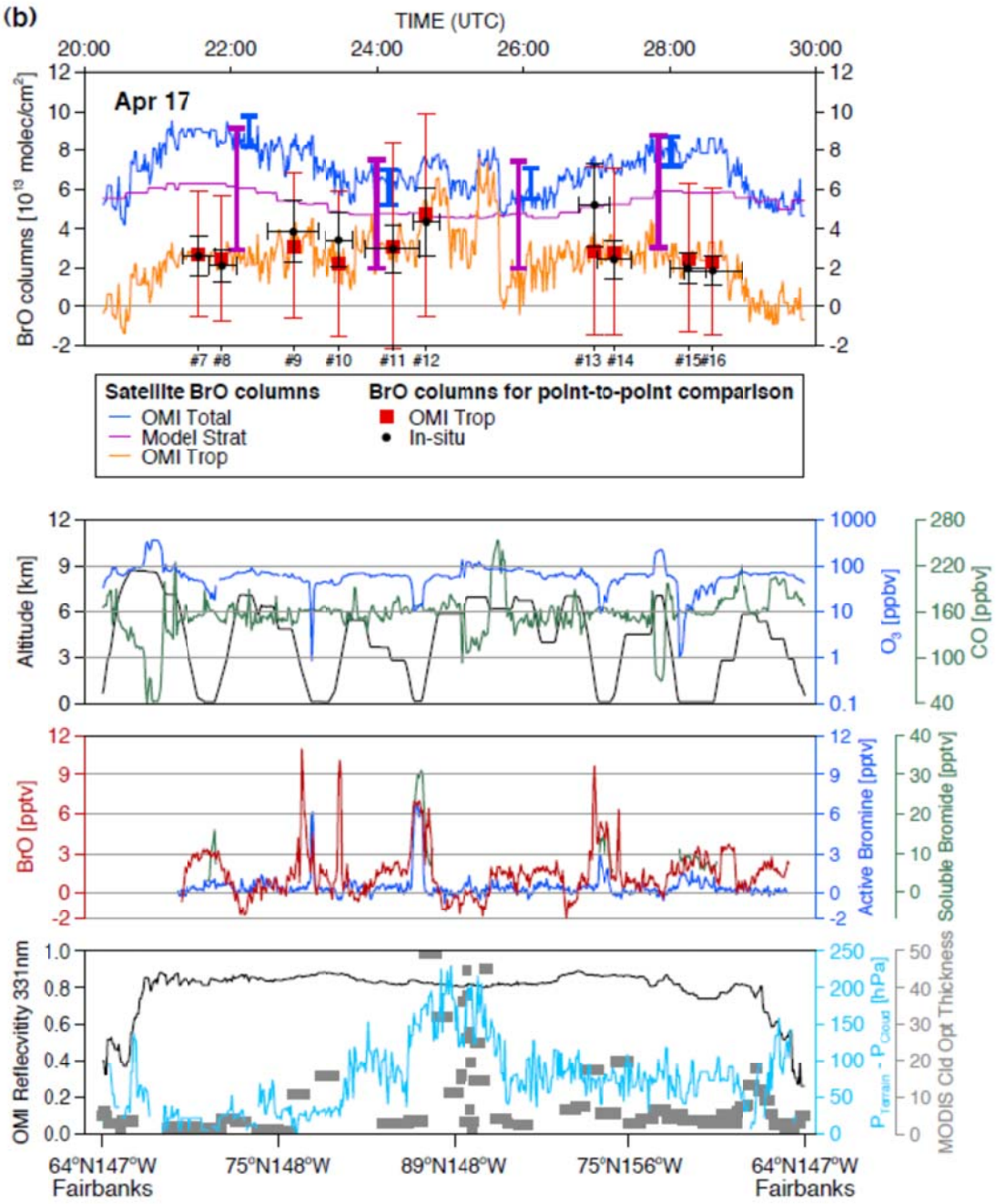


**Figure 1.** Time series plots of OMI total, model stratospheric and OMI-model tropospheric VCD BrO, accompanied by time series of ozone, CO, BrO, active bromine, soluble bromide, OMI reflectivity at 331 nm, the difference between effective cloud pressure and terrain pressure, and MODIS cloud optical thickness on 17 April 2008.

Satellite-derived BrO tropospheric columns (orange line) are about zero near Fairbanks (see top panel of Fig. 1). Tropospheric BrO information is not reliably retrieved when surface reflectivities are less than approximately 0.4, which is the case near Fairbanks (see the fourth panel of Fig. 1). Both total and tropospheric column BrO show a slight dip near the pole, where the OMI and MODIS cloud products indicate shielding clouds (middle of Fig. 1). Here, the low values of derived tropospheric BrO over optically thick clouds likely result from the cloud shielding effect [Theys et al., 2011]. Such clouds may also reduce tropospheric BrO columns by slowing photochemical production of active bromine.

On the other hand, high values of satellite-derived tropospheric column are found along the DC-8 flight path both before the descent in altitude at approximately 24:15 UTC and after the plane has ascended. Data from both OMI and MODIS indicate optically thick clouds were present during and after the ascent. The high value of satellite-derived tropospheric column during and after ascent could be due to the presence of BrO above or within these clouds. Profile #12 shows a plume of enhanced BrO at about 3 km altitude, which could have been above the cloud deck. In-situ tropospheric column BrO, marked as black dots in the time series plot (the first panel of Fig. 1), are obtained by integrating in-situ BrO mixing ratio profiles. Uncertainties in the in-situ columns are shown as black vertical error bars. The horizontal bars indicate the distance covered by corresponding flight ascents/descents. OMI tropospheric BrO columns for point-to-point comparisons with aircraft data, shown as red squares, are obtained by averaging pixels over the corresponding flight segment.

The OMI tropospheric BrO columns exhibit a magnitude and variability similar to that of the DC-8 in-situ columns. For example, profile #12 reports high BrO mixing ratios from the surface to 4 km; the OMI tropospheric BrO column is also relatively high at the same location.

However, some discrepancies appear, perhaps because the aircraft captures small scale features that the satellite observations cannot resolve. For example, in-situ profile #13 shows a relatively large value for tropospheric column BrO, caused by enhanced BrO mixing ratios in a layer near 2 km. This could be a local event as the nearby aircraft column #14 does not show such an enhancement. The satellite retrieval agrees well with profile #14 but underestimates the abundance of BrO measured in profile #13. Overall, OMI tropospheric column BrO quantitatively agrees with the DC-8 in-situ column BrO to within the respective estimated uncertainties. The comparison between satellite and in-situ tropospheric column BrO for this flight is further quantified by Liao et al. [2011]. These comparisons demonstrate the ability of OMI to capture the magnitude and spatial distribution of tropospheric column BrO over bright surfaces for clear conditions.

## 3. BrO explosion event observed from OMI

Events of rapid enhancement of tropospheric column BrO are apparent from OMI observations after adjustment for the stratospheric burden of BrO, for the time period mid-March to late April 2008. The NASA DC-8 aircraft flew into an area of enhanced tropospheric column BrO near the North Pole on 17

April 2008 and the NOAA WP-3D aircraft flew near another tropospheric BrO enhancement on 19 April 2008. Here we examine the event near the North Pole on 17 April 2008 and similar events in more detail using only OMI retrievals. The wide orbital swath and high spatial resolution of OMI, in addition to its frequent observations at high latitudes, provide a unique view of the temporal evolution of these events.

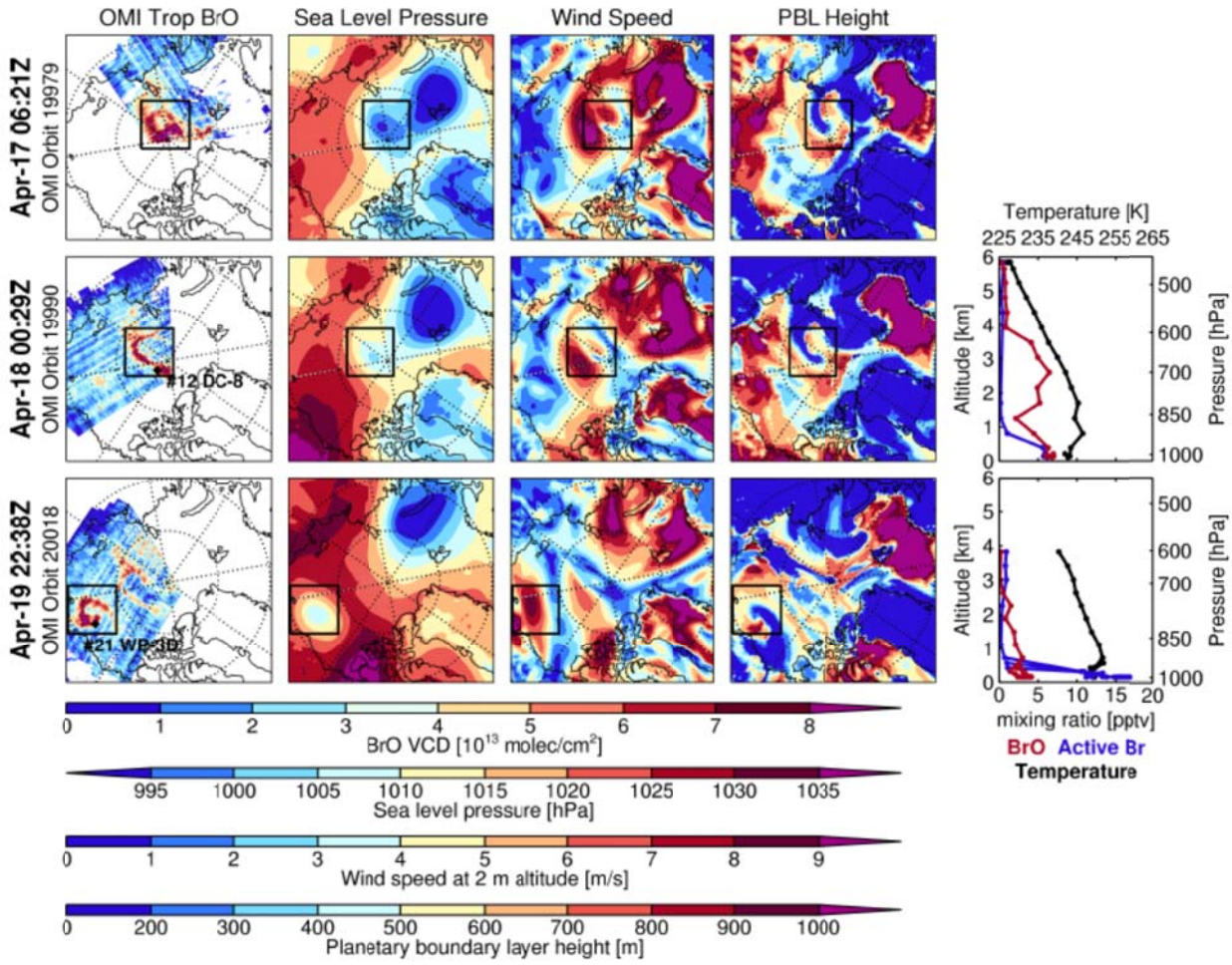


**Figure 2.** First column: OMI tropospheric BrO VCD; Second column: MERRA sea level pressure; third column: MERRA wind speed at 2m altitude; fourth column: MERRA planetary boundary layer height; fifth column: aircraft in-situ profiles of BrO (red), active bromine (blue) and temperature (black). The rows correspond to OMI orbits. We show results for orbit 19979 on 17 April 2008 (top row), orbit 19990 on 18 April 2008 (middle row), and orbit 20018 on 19 April 2008 (bottom row). Aircraft profiles were not obtained during the time that the satellite data shown in the top row were acquired.

Figure 2 shows three tropospheric BrO enhancement events during April 2008 along with maps of sea level pressure, wind speed at 2m altitude, and planetary boundary layer height from MERRA for the closest synoptic hour. For these events, the locations of enhanced BrO columns are coincident with high

near-surface wind speeds (3rd column) that are geostrophically consistent with localized low pressure systems. Neuman et al. [2010] also note high wind speed along the flight paths in conjunction with high concentrations of active bromine. Our analysis is consistent with the suggestion that strong surface winds associated with low pressure systems can trigger bromine activation via blowing snow [Yang et al., 2008, 2010, Jones et al., 2009, 2010].

Figure 2 also shows that the spatial structure of high tropospheric column BrO is similar to that of the planetary boundary layer (PBL) height, although there is not always a precise alignment of these features. At high latitudes where the meteorological analysis is driven primarily by satellite data, the MERRA fields may contain displacement or other errors, particularly in near-surface fields. The following discussion should therefore be considered somewhat speculative in light of these uncertainties. We provide an animated visualization as a Supplement to depict evolution of enhanced tropospheric column BrO, sea level pressure, wind speed at 2m and planetary boundary layer height from 16 to 18 April 2008.

The second row of Fig. 3.16 illustrates an event at 00:30 UTC on 18 April 2008 and the third row is for an event at 22:40 UTC on 19 April 2008. The two OMI orbits presented are closest in time to airplane flights into the elevated BrO and active bromine layers. The locations of the profiles are shown as black diamonds on the maps of tropospheric BrO. The aircraft profiles of temperature, BrO mixing ratio, and active bromine mixing ratio are presented in the last column. Aircraft measurements show enhanced active bromine in the near-surface layer for both flights and enhanced amounts of BrO for the 18 April flight. Satellite-derived tropospheric BrO enhancements are closely related to near-surface parameters including sea level pressure, wind speed at 2 m, and PBL height. This observation suggests that the BrO activations originate at the surface, which of course is consistent with prior expectation. For the event on 18 April, a tail of enhanced BrO column exists parallel to the wind direction inferred from sea level pressure. Begoin et al. [2010] suggested long range transport of tropospheric inorganic bromine for plumes in which recycling of bromine from condensed to gas phase sustains elevated BrO. The profile for BrO measured on 18 April by the DC-8 instrument (Fig. 3.16) also shows enhancements in the free troposphere, above the top of the PBL height (about 500 m). Simultaneous profiles of CO and O3 (not shown in Fig.2, see Fig. 1) imply no stratospheric influence. The existence of elevated BrO above the top of the PBL could be due to vigorous convection over ice leads driven by warm exposed water, with BrO then dispersed horizontally by prevailing winds [Simpson et al., 2007b, Salawitch et al., 2010]. Our results are consistent with a surface origin of elevated BrO as well as transport of inorganic bromine-enriched air parcels away from the source of origin.

## 4. Free tropospheric abundance of BrO derived from cloud slicing

Cloud slicing technique takes advantage of opaque nature of optically thick clouds to estimate a volume mixing ratio of a trace gas in the free troposphere [Ziemke et al., 2001]. As optically thick clouds are opaque at the wavelength range of BrO retrieval, the column amount BrO measured by OMI in the presence of such clouds is “above-cloud” column of BrO (from cloud pressure to the top of atmosphere

(TOA)). We combine collocated measurements of OMI above-cloud column BrO and cloud scene pressure to yield BrI profile information.

We use the cloud slicing technique to obtain monthly climatology of free tropospheric BrO volume mixing ratio (VMR) using OMI data from Oct 2004 to Apr 2008. These maps are obtained for a 5 degree latitude x 5 degree longitude grid over the globe. For each grid box, we fit the observed BrO column over clouds versus effective cloud scene pressure (Pscene) using simple linear regression, i.e.,

VCD (from Pscene to TOA) = A x Pscene + B

BrO VMR can be obtained from the slope, A, of this fit using

BrO VMR (pptv)= 417.7 x A

where the unit of A is $10^{13}$ molecules $cm^{-2}$ per hPa. OMI pixels with an effective cloud fraction > 0.7 and reflectivity > 0.6 are used for this calculation where cloud retrievals are most accurate [Joiner et al., 2012] and sensitivity to tropospheric BrO is highest [Theys et al., 2011, Choi et al., 2012]. The BrO VMR obtained is valid for the range of altitudes spanned by Pscene and assumes vertical homogeneity within that range. We also assume that both stratospheric column BrO and tropospheric mean BrO VMRs are not highly variable over a given ensemble grid box and time period (1 month).

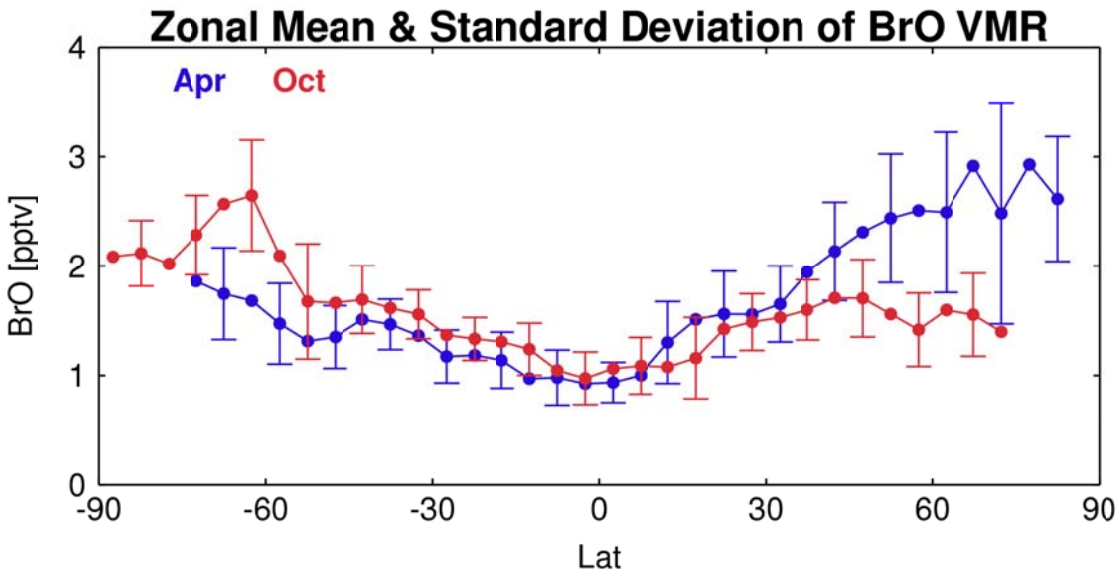


**Figure 4.** Zonal mean and standard deviation of BrO VMR as a function of latitude for April 2005-2008 (blue) and for October 2004-2007 (red). The standard error of the mean (not shown) is less than 0.1 pptv in most regions except polar regions, and is less than 0.2 pptv in polar regions.

Figure 4 shows the zonal mean and standard deviation of BrO VMR calculated for 5 degree binned zonal bands. The standard deviation is shown for every 10 degrees. The standard error of the mean (not shown) is less than 0.1 pptv in most regions except in polar regions, and is less than 0.2 pptv in polar

regions. In the tropics, BrO VMR is almost constant at about 1 pptv, but BrO VMR is slightly higher in spring in both hemispheres. This trend is appears in mid-latitudes as well. During springtime in the northern hemisphere, free tropospheric BrO is enhanced in wide regions at latitudes between 45 degree N and 80 degree N. On the other hand, in the southern hemisphere, a sharp peak of enhanced BrO in springtime (October) is centered at 65 degree S, possibly connected with BrO activation in the coastline of the Antarctica. As described in previous paragraph, small peaks of BrO VMR in fall are apparent near 40 latitude in fall of both hemispheres. Relatively high BrO VMR are maintained in autumn at the regions of polar BrO activation.

**References**


Ariya, P., Dastoor, A. P., Amyot, M., Schroeder, W. H., Barrie, L., Anlauf, K.,Rao_e, F., Ryzhkov, A., Davignon, D., Lalonde, J., and Ste_en, A.: The Arctic: a sink for mercury, Tellus, 56B, 397-403, 2004.

Barrie, L. A., Bottenheim, J. W., Schnell, R. C., Crutzen, P. J., and Rasmussen, R. A.: Ozone destruction and photochemical reactions at polar sunrise in the lower Arctic atmosphere, Nature, 334, 138-141, 1988.

Begoin, M., Richter, A., Weber, M., Kaleschke, L., Tian-Kunze, X., Stohl, A., Theys, N., and Burrows, J. P.: Satellite observations of long range transport of a large BrO plume in the Arctic, Atmos. Chem. Phys., 10, 6515-6526, doi:10.5194/acp-10-6515-2010, 2010.

Bovensmann, H., Burrows, J. P., Buchwitz, M., Frerick, J., No el, S., Rozanov, V. V., Chance, K. V., and Goede, A. P. H.: SCIAMACHY: Mission Objectives and Measurement Modes, J. Atmos. Sci., 56, 127-150, 1999.

Chance, K.: Analysis of BrO Measurements from the Global Ozone Monitoring Experiment, Geophys. Res. Lett., 25, 3335-3338, 1998.

Choi, S., Wang, Y., Salawitch, R. J., Canty, T., Joiner, J., Zeng, T., Kurosu, T. P., Chance, K., Richter, A., Huey, L. G., Liao, J., Neu- man, J. A., Nowak, J. B., Dibb, J. E., Weinheimer, A. J., Diskin, G., Ryerson, T. B., da Silva, A., Curry, J., Kinnison, D., Tilmes, S., and Levelt, P. F.: Analysis of satellite-derived Arctic tropospheric BrO columns in conjunction with aircraft measurements during ARCTAS and ARCPAC, Atmos. Chem. Phys., 12, 1255-1285, 2012.

Hegels, E., Crutzen, P. J., Klupfel, T., Perner, D., and Burrow, J. P.: Global distribution of atmospheric bromine-monoxide from GOME on earth observing satellite ERS-2, Geophys. Res. Lett., 25, 3127-3130, 1998.

Joiner, J., Yoshida, Y., Vasilkov, A. P., Middleton, E. M., Campbell, P. K. E., Yoshida, Y., Kuze, A., and Corp, L. A.: Filling-in of far-red and near-Infrared solar lines by terrestrial and atmospheric e_ects: simulations and space-based observations from SCIAMACHY and GOSAT, Atmos. Meas. Tech., 5, 809-829, 2012.

Levelt, P. F., van den Oord, G. H. J., Dobber, M.R., M alkki, A., Visser, H., de Vries, J., Stammes, P., Lundell, J., and Saari, H.: The Ozone Monitoring Instrument, IEEE T. Geosci. Remote Sens., 44, 1093-1101, doi:10.1109/TGRS.2006.872333, 2006.

Liao, J. Huey, L. G., Scheuer, E., Dibb, J. E. Stickel, R. E., Tanner, D. J., Neuman, J. A., Nowak, J. B., Choi, S., Wang, Y., Joiner, J., Salawitch, R. J., Canty, T., Weinheimer, A. J., Shetter, R. E., Fried, A., Brune, W., Anderson, B., Zhang, W., Chen, G., Crawford, J., and Hecobian, A.: Characterization of soluble bromide measurements and a case study of BrO observations during ARCTAS, Atmos. Chem. Phys., 12, 1327-1338, 2012.

Munro, R., Eisinger, M., Anderson, C., Callies, J., Corpaccioli, E., Lang, R., Lefebvre, A., Livschitz, Y., and Albinana, A. P.: GOME-2 on MetOp, in: Proc. of The 2006 EUMETSAT Me- teorological Satellite Conference, Helsinki, Finland, 12-16 June 2006, EUMETSAT, p. 48, 2006.

Neuman, J. A., Nowak, J. B., Huey, L. G., Burkholder, J. B., Dibb, J. E., Holloway, J. S., Liao, J., Peischl, J., Roberts, J. M., Ryerson, T. B., Scheuer, E., Stark, H., Stickel, R. E., Tanner, D. J., and Weinheimer, A.: Bromine measurements in ozone depleted air over the Arctic Ocean, Atmos. Chem. Phys., 10, 6503-6514, doi:10.5194/acp-10-6503-2010, 2010.

Read, K. A., Majahan, A. S., Carpenter, L. J., Evans, M. J., Faria, B. V. E., Heard, D. E., Hopkins, J. R., Lee, J. D., Moller, S. J., Lewis, A. C., Mendes, L., MaQuaid, J. B., Oetjen, H., Saiz-Lopez, A., Pilling, M. J., and lane, J. M. C.: Extensive halogen-mediated ozone destruction over the tropical Atlantic Ocean, Nature, 453, 1232-1235, 2008.

Richter, A., Wittrock, F., Eisinger, M., and Burrows, J. P.: GOME Observations of Tropospheric BrO in Northern Hemispheric Spring and Summer 1997, Geophys. Res. Lett., 25, 2683-2686, 1998.

Saiz-Lopez, A., Shillito, J. A., Coe, H., and Plane, J. M. C.: Measurements and modelling of I2, IO, OIO, BrO and NO3 in the mid-latitude marine boundary layer, Atmos. Chem. Phys., 6, 1513-1528, 2006.

Salawitch, R., Canty, T., Kurosu, T., Chance, K., Liang, Q., da Silva, A., Pawson, S., Nielsen, J. E., Rodriguez, J. M., Bhartia, P. K., Liu, X., Huey, L. G., Liao, J., Stickel, R. E., Tanner, D. J., Dibb, J. E., Simpson, W. R., Donohoue, D., Weinheimer, A., Flocke, F., Knapp, D., Montzka, D., Neuman, J. A., Nowak, J. B., Ryerson, T. B., Oltmans, S., Blake, D. R., Atlas, E. L., Kinnison, D. E., Tilmes, S., Pan, L. L., Hendrick, F., Van Roozendael., M., Kreher, K., Johnston, P. V., Gao, R. S., Johnson, B., Bui, T. P., Chen, G., Pierce, R. B., Crawford, J. H., and Jacob, D. J.: A new interpretation of total column BrO during Arctic spring, Geophys. Res. Lett., 37, L21805, doi:10.1029/2010GL043798, 2010.

Schroeder, W. H., Anlauf, K. G., Barrie, L. A., Lu, J. Y., Ste_en, A., Schneeberger, D. R., and Berg, T.: Arctic springtime depletion of mercury, Nature, 394, 331-332, 1998.

Simpson, W. R., von Glasow, R., Riedel, K., Anderson, P., Ariya, P., Bottenheim, J., Burrows, J., Carpenter, L. J., Frie_, U., Goodsite, M. E., Heard, D., Hutterli, M., Jacobi, H.-W., Kaleschke, L., Ne_, B., Plane, J., Platt, U., Richter, A., Roscoe, H., Sander, R., Shepson, P., Sodeau, J., Ste_en, A., Wagner, T., and Wol_, E.: Halogens and their role in polar boundary-layer ozone depletion, Atmos. Chem. Phys., 7, 4375-4418, doi:10.5194/acp-7-4375-2007, 2007.

Theys, N., Van Roozendael, M., Errera, Q., Hendrick, F., Daerden, F., Chabrillat, S., Dorf, M., Pfeilsticker, K., Rozanov, A., Lotz, W., Burrows, J. P., Lambert, J.-C., Goutail, F., Roscoe, H. K., and De Mazi_ere, M.: A global stratospheric bromine monoxide climatology based on the BASCOE chemical transport model, Atmos. Chem. Phys., 9, 831-848, doi:10.5194/acp-9-831-2009, 2009.

Theys, N., Van Roozendael, M., Hendrick, F., Yang, X., De Smedt, I., Richter, A., Begoin, M., Errera, Q., Johnston, P. V., Kreher, K., and De Mazi_ere, M.: Global observations of tropospheric BrO columns using GOME-2 satellite data, Atmos. Chem. Phys., 11, 1791{1811, doi:10.5194/acp-11-1791-2011, 2011.

Toumi, R: BrO as a sink for dimethylsul_de in the marine atmosphere, Geophys. Res. Lett., 21, 117-120, 1994.

von Glasow, R., von Kuhlmann, R., Lawrence, M. G., Platt, U., and Crutzen, P. J.: Inpact of reactive bromine chemistry in the troposphere, Atmos. Chem. Phys., 4, 2481-2497, 2004.

Wagner, T. and Platt, U.: Satellite mapping of enhanced BrO concentrations in the troposphere, Nature, 395, 486-490, 1998.

Ziemke, J. R., Chandra, S., and Bhartia, P. K.: \Cloud Slicing": A new technique to derive upper tropospheric ozone from satellite measurements, J. Geophys. Res., 106, 9853-9867, 2001.